OPEN ACCESS

ACTA METALLURGICA SLOVACA

2025, VOL. 31, NO. 3, 181-185

RESEARCH PAPER

The effect of adding Mn and Cr to the Al-Fe-Si system alloy

Violetta Andreyachshenko[1,], Marat Ibatov[2], Ainagul Toleuova[3]*

v.andreyachshenko@ktu.edu.kz, [2]Imaratk@mail.ru, [3] rymkul.ainagul@mail.ru

*Corresponding author: v.andreyachshenko@ktu.edu.kz, tel.: 87013962994, Abylkas Saginov Karaganda Technical University, Nursultan Nazarbayev Avenue No. 56, 100027, Karaganda, Kazakhstan

Received: 29.07.2025
Accepted: 08.08.2025

ABSTRACT

Alloys of the Al-Fe-Si system have a complex phase composition that determines their properties. With a certain combination of temperature and composition, the conditions for the formation of the α phase are formed. However, with decreasing temperature, the α↔β transformation is observed. Suppression of the formation of the β phase is possible by doping. The main goal of this work was to substantiate theoretically the introduction of manganese and chromium into the alloy and to explain the required number of alloying elements through a detailed analysis of the phase composition. The temperature limits for the formation of the α phase in the Al-Fe-Si ternary system and the kinetics of its recrystallisation were revealed. A justification for the value of the mass fraction of alloying elements that contribute to the suppression of the α↔β transformation with the formation of the cubic α phase was developed. The most successful suppression of the formation of the β phase occurs with joint alloying with manganese and chromium, with the formation of a predominantly cubic phase $Al_{15}Si_2(Fe, Cr, Mn)_4$ with a volume fraction of more than 95%, which predicts the possibility of plastic processing of iron and silicon-rich alloys of the Al-Fe-Si system.

Keywords: Al-Fe-Si; α phase; β phase; Thermo Calc; phase diagram

INTRODUCTION

Alloys of the Al-Si system are the most popular aluminum alloys that are widely used in various industries [1-6]. In such alloys, iron impurities are harmful. The essence of the harmful effect of iron is the formation of needle- and plate-shaped intermetallic phases that reduce both the strength and plastic properties of the alloy. It is possible to minimise the harmful effects of iron by alloying with various elements such as Mn, Cr, B and others. It has been proven that the addition of Mn suppresses the formation of the β phase with the formation of the cubic intermetallic phase α-Al(Mn,Fe)Si. Cr additions and co-doping of Cr and Mn have a similar effect, binding iron into cubic intermetallic compounds of the α-AlFeMnCrSi type.

However, most of the works deal with studying additives to Al-Si iron-containing alloys with the iron content of 0.1-2%. Alloys with high iron content are of greater interest, since they can exhibit increased mechanical properties, while remaining alloys with a reduced density [7-11]. The results of work [12] indicate increasing the crystallisation temperature of iron-containing phases with the addition of manganese, as well as manganese and silicon together. The authors note that the addition of Mn to the Al-Fe-Si system leads to the formation of the τh phase instead of the θ-Al3Fe phase with the iron content of more than 10.3%. The τh phase has a hexagonal crystal structure P63/mmc) [13]. In work [14], the effect of Mn and Mo alloying of the Al-Si-Cu alloy was studied, and the transition of the θ phase to α-Al(FeMnMo)Si was discovered; however, no information was provided on the effect of copper on the phase formation. Works [15, 16] report that the actual mechanism of suppressing the formation of the β phase in favor of the α phase is accelerated cooling. The addition of cobalt and manganese can replace iron atoms, resulting in the transformation of the needle-shaped structure into a cubic or hexagonal shape. Empirically, the determined optimal ratio of Co and Fe in intermetallic compounds having Chinese script with the hexagonal structure is 1–2 [17], and the ratio of Mn and Fe is 0-1:1 [18] with increased cooling rates. At the same time, it was noted in work [19] that Mn additions in the Al–Si–Cu–Fe alloy led to the settling of iron-enriched intermetallic particles in the α- $Al_{15}(Fe,Mn)_3Si_2$ modification to the bottom of the crucible, thereby leading to purification of the alloy from iron. In this case, the crystal structure of α-Al(Mn,Fe)Si changes from body-centred cubic (bcc)/simple cubic structure to the Pm3 structure with increasing the volumetric Mn content in the alloy [20].

At the same time, in work [21] it is noted that the monoclinic β-Al5FeSi phase is not a feature of the pure Al-Si-Fe system, since it was not found in any of the alloys studied by the authors, unlike industrial alloys containing additional impurities (Mn, Cr, Cu, P).

MATERIAL AND METHODS

There were studied the Al_{60}-Fe_{30}-Si_{10}, $Al_{60} – Fe_{30-x} – Si_{10} – Mn_x$ and $Al_{60} – Fe_{30-x} – Si_{10} – Cr_x$ alloys. For alloys simultaneously alloyed with chromium and manganese, the ratio Al=60%-const, Si=10%-const, Σ(Fe, Cr, Mn)=30% was used. Numerical modelling to study the phase composition of the three-component system was carried out using the ThermoCalc software. As part of the study, the Al-Fe-Si system under study was specified for calculation. An important element of the calculations is the identification and assessment of the interaction of the system's main components. Aluminum was selected as the base material, because its quantity in the system is maximum. The ThermoCalc software version 2024a, the TCAL8 database, version v8.2, were used for modelling. Such tools as the Phase diagram, the One Axis, the Scheil Solidification, and the Ternary calculation were used for the calculation.

RESULTS AND DISCUSSION

Al-Fe-Si ternary phase diagram

In the Al-Fe-Si ternary diagram (**Fig. 1**), the position of the liquidus line is determined by the mass content of iron. The polythermal section with the aluminum content of 60 wt. % and variable amounts of silicon and iron are of interest. When the silicon content is more than 30 %, particles of primary silicon are released from the liquid phase. After depletion of the liquid phase, it becomes possible to form the intermetallic phase τ_4 that belongs to the tetragonal system. With decreasing the temperature, it transforms into the β phase with a monoclinic crystal lattice by isothermal reaction. The τ_4↔β transition ends with the complete disappearance of the liquid phase with crystallization of the fcc solid solution of silicon and iron in aluminum (Al), thereby forming a solidus line at the temperature of 571 °C. With the Fe/Si ratio of ~1/1 or more, the primary phase becomes the τ_2 phase, the structure of which has not yet been unambiguously determined. Still, some researchers attribute it to the triclinic system. From ~25 % iron, the primary phase is the θ phase, precipitation of which determines the liquidus line. Then, according to the reaction L+θ↔ L+θ+τ_2, the τ_2 phase begins to separate from the liquid. When the iron content is 24-39 %, and the silicon content is 1-16 %, the conditions for precipitation of α-phase crystals are formed at temperatures below 770 °C. Thermodynamically possible conditions for the existence of the α phase are limited to a temperature of 425 °C. With a further decrease, a complete transformation of α↔β occurs. At the room temperature the alloy consists entirely of the β phase, and at varying silicon and iron contents it is accompanied by a low symmetry τ_8 phase, an acicular θ phase, primary silicon (Si), or a small amount of fcc aluminum. The results obtained are in good agreement with previously conducted studies [22].

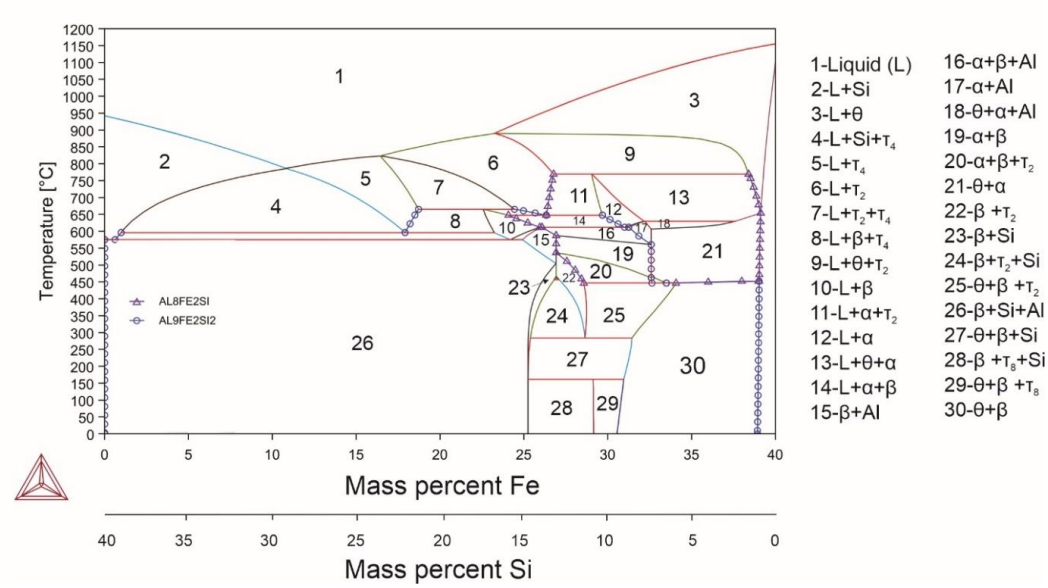

Fig. 1 Phase diagram of the Al-Fe-Si system state

Such a phase composition of the alloy of the Al-Fe-Si system that is rich in both silicon and iron, excludes the possibility of deformation processing of the resulting alloy. To improve the ability to tolerate plastic deformation, it is necessary to develop effective methods of suppressing the α↔β transformation.

Adding Mn to the Al-Fe-Si system

A priori [23-26], the positive effect of manganese on the suppression of the α↔β transition is known; however, most works are limited to metallographic studies without sufficient theoretical justification for selecting the quantitative factor when doping with manganese. It was decided to consider the effect of manganese on the formation of the α phase. **Fig. 2** shows a polythermal section of the Al-Fe-Si-Mn system with varying contents of manganese, iron and silicon.

Crystallisation of the alloy begins with phase θ#2 at a temperature of ~880 °C. This phase has a monoclinic crystal lattice and its primary crystals tend to grow along the [010] orientation, forming rough needles, flakes and plate-shaped forms, which significantly degrade the mechanical properties of the alloys.

In this system, three three-phase reactions involving fcc (Al) occur: L + α_{Mn} + β → β + α_{Mn} + α + (Al); α_{Mn} + β → β + α_{Mn} + (Al); α_{Mn} + (Al) → β + α_{Mn} + α + τ_2. Here, it is worth noting the formation of the α_{Mn} phase throughout almost the entire section area. There are three ternary compounds in equilibrium with (Al): Al8Fe2Si (α), $Al_{15}Si_2Mn_4$ (α_{Mn}) and $Al_9Fe_2Si_2$ (β). Moreover, the Al_8Fe_2Si (α) phase has a rather narrow crystallisation range and transforms into the $Al_9Fe_2Si_2$ phase as the temperature decreases, which is a very undesirable process. The presence of the $Al_9Fe_2Si_2$ phase in the structure entails deterioration in the mechanical properties of the material.

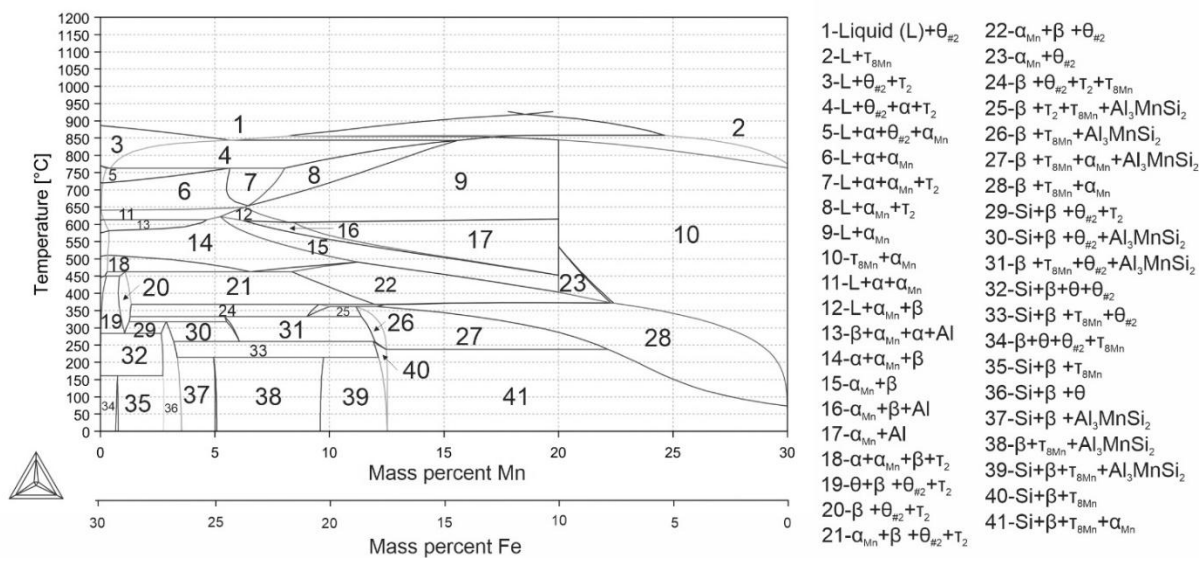

Fig. 2 Polythermal section of the Al-Fe-Si-Mn system

Crystallisation of the α phase occurs with the manganese content of up to 8 %, and iron up to 25 % inclusive. According to the phase diagram, complete suppression of the α↔β transition by doping with manganese cannot be achieved. Still, it is possible to form an intermetallic compound in which some of the iron atoms are replaced by manganese atoms, designated as the α_{Mn} phase and having a cubic crystal lattice. The α_{Mn} phase is more thermally stable and is detected down to room temperatures with a certain ratio of the components of the system. Thus, when the manganese content is up to 10%, the β phase crystallises. Already when the manganese content increases from 10 to 30 %, the formation of the β phase is suppressed by the formation of the α_{Mn} phase, which is the most favorable, since the α_{Mn} phase has a cubic lattice, optimal for further deformation of the alloy.

Adding Cr to the Al-Fe-Si system

Another common element that can suppress the formation of the β phase is chromium [27-30]. Therefore, it was decided to consider the effect of chromium on the formation of the α phase. **Fig. 3** shows a polythermal section of the Al-Fe-Si-Cr system with varying contents of chromium, iron and silicon.

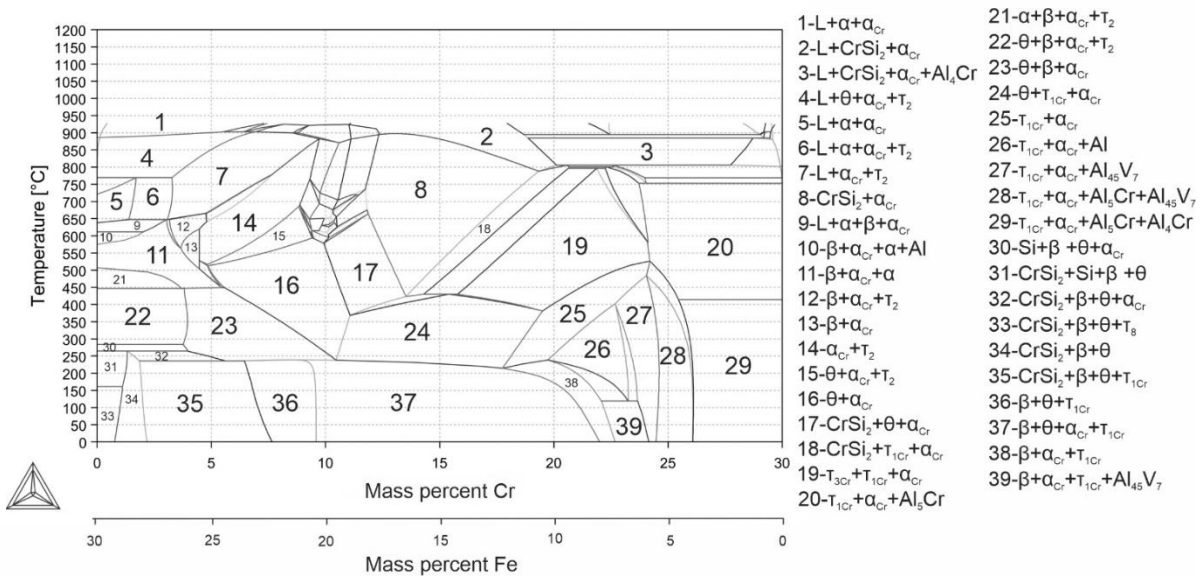

Fig. 3 Polythermal section of the Al-Fe-Si-Cr system

Under equilibrium conditions, solid solutions and intermetallic compounds begin to crystallise simultaneously from the liquid solution. The α phase crystallises by the eutectic reaction L → α_{Cr} + α at the temperature of ~880 °C. As in the case of manganese, the α phase has a narrow crystallisation range. The α_{Cr} phase is formed by analogy with the α_{Mn} phase, when in an intermetallic compound, some of the iron atoms are replaced by chromium atoms, and has a cubic crystal lattice. The α_{Cr} phase has a fairly wide crystallisation range, in contrast to the α phase. It can be assumed that the appearance of primary crystals of the α_{Cr} phase suppresses the appearance of the θ phase, which is formed in region four at a temperature of ~895 °C. The θ phase is formed by the peritectic reaction L + $CrSi_2$ + α_{Cr} → θ + α_{Cr} + τ_2 at the temperature of 997 °C.

The θ phase, or $Al_{13}Fe_4$, like the $\theta_{\#2}$ phase belongs to the monoclinic system. It should be noted that the formation of this phase in the form of needle-shaped particles sharply reduces the technological ductility of aluminium alloys. Silicon is added to prevent the formation of θ - phase particles and to ensure precipitation of the Al_8Fe_2Si phase into the alloy.

In the iron content range from 10 to 20 %, the formation of the β phase is also suppressed by the formation of the α_{Cr} phase. This is a favorable factor, since the cubic phase α_{Cr} predicts susceptibility of the alloy to plastic deformation.

Quantitative estimation of the phase composition

A better understanding of the phase composition characteristics of an alloy of the Al–Fe–Si system with Mn and Cr is achieved by considering the ratio of the phases formed during alloying. The expediency of choosing the number of alloying additives is determined by the peculiarities of the patterns of redistribution of the number of phase components during alloying. The determining factors in the formation of the phase composition are the number of elements included in the alloy, and depending on the temperature, the alloy can significantly change its phase composition even with an identical composition. Using the One Axis tool, the volume fraction of all the phases formed in a given temperature range was estimated. Three points were selected as representative temperatures: the average solidus temperature is 600 °C, as well as the temperatures of 500 °C and 400 °C. The operating temperatures of heat-resistant aluminum alloys were 250-350 °C. Therefore, to ensure stability of properties at these temperatures, it was necessary to fix the composition and properties at higher processing temperatures. The estimation was carried out by doping the alloy with the base composition of $Al_{60} – Fe_{30-x} – Si_{10}$ with iron atoms. Thus, there were considered alloys with the composition $Al_{60} – Fe_{30-x} – Si_{10} – Mn_x$ and $Al_{60} – Fe_{30-x} – Si_{10} – Cr_x$, with x=1, 5, 10 and 15 %. **Fig. 4** shows the phase composition relative to the α, αMn/Cr, β phases. The remaining phases are shown collectively as the other phases.

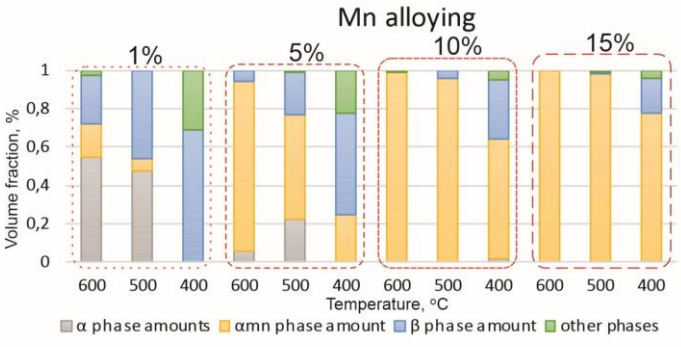

Fig. 4 Quantitative estimation of the phase composition with Mn

Chemical and phase composition

Previous studies of the three-component Al-Fe-Si system showed that the alloy with the composition $Al_{60}Fe_{30}Si_{10}$ in wt. % has a preferable composition among

the alloys of this system, which is rich in both iron and silicon [27]. At the same time, the charge materials used are not pure, so additional chemical elements inevitably end up in the finished alloy during synthesis. Besides, the flux, in addition to protecting the metal bath from oxidation, also meets the molten metal, making certain adjustments to the basic (planned) chemical composition.
It was revealed that the α_{Mn} phase was formed even when doped with 1% manganese. As a result, at 600 °C, the α phase was predominantly detected, with approximately equal amounts of the α_{Mn} and β phases. When cooled to 500 °C, the α↔β transformation was observed with the decrease in the αMn phase, and already at 400 °C, the highly symmetrical phases completely recrystallise into phases of lower symmetries. With increasing the amount of manganese, suppression of the α↔β transition is observed with the formation of a predominantly cubic α_{Mn} phase even at 400 °C.
When doped with chromium, suppression of the α↔β transition is observed even with the addition of 5 % chromium. The addition of 10 % chromium (**Fig. 5**) eliminates both the β and α phases with the formation of a certain amount of some phases that can also be strengtheners. It is worth noting that the $Al_{60} – Fe_{25} – Si_{10} – Cr_5$ alloy consists entirely of the α_{Cr} phase at 600 and 500 °C.

Adding Cr and Mn to the Al-Fe-Si system

Considering the positive effect of doping the Al-Fe-Si system alloy separately with chromium and manganese, it is logical to assume that the impact can be enhanced by simultaneous doping with both elements. To more effectively find a solution, the principle of experiment planning was used.
In this study, the total number of α phases is taken as the optimisation parameter. The number of phases was determined when implementing the experiment in the ThermoCalc software package.

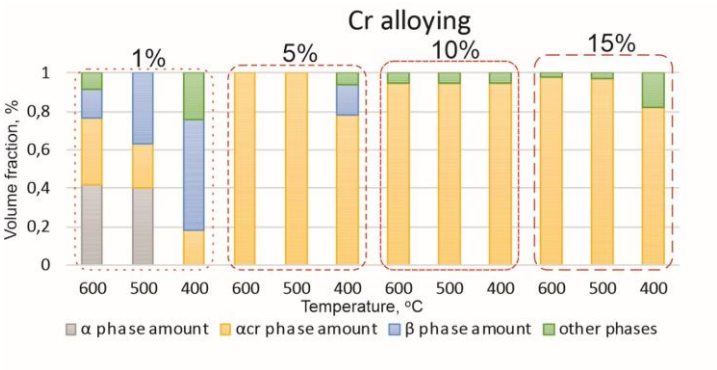

Fig. 5 Quantitative estimation of the phase composition with Cr

In this case, as a result of doping simultaneously with the Mn and Cr components, recrystallization of the α and β phases was observed with the formation of the $Al_{15}Si_2M_4$ phase, where M is a combination of Fe, Cr and Mn atoms; thus the formed phase is written as $Al_{15}Si_2M_4$, it belongs to the cubic system, thereby predicting the ability to perceive plastic deformation. Therefore, the mathematical model can be written as Σα=f(T, Fe, Cr, Mn, Si, Al).
According to the rule of independence of factors, it is impossible to vary all the six factors simultaneously, therefore, it was decided to conduct tests at Al=60%-const, Si=10%-const, varying manganese and chromium was carried out due to the iron content, subject to the fulfillment of the condition Σ(Fe , Cr, Mn)=30%.
This approach is associated with the interchangeability of iron, chromium and manganese atoms during the formation of the $Al_{15}Si_2M_4$ phase.
The conditions for encoding factors are shown in **Table 1**. It shows the initial data used in setting up the numerical experiment.

Table 1 Chemical composition of the synthesized alloy

No.	Temperature, °C	Alloy composition, wt %					Volume fraction of $\alpha_{Mn/Cr}$, %
		Al	Fe	Si	Mn	Cr	
1	600	60	95	10	10	10	95
2	600	60	99	10	10	1	99
3	600	60	98	10	1	10	98
4	600	60	82*	10	1	1	82*
5	400	60	68	10	10	10	68
6	400	60	75	10	10	1	75
7	400	60	98	10	1	10	98
8	400	60	20	10	1	1	20

*including the α-27% phase

Considering that the experiment was carried out under the conditions of a numerical experiment, when it was repeated, completely identical indicators were obtained, which indicates the impossibility of duplicating experiments. Therefore, it was not possible to determine confidence intervals for the model coefficients. Considering the results of alloying with chromium and manganese separately, the assumption can be accepted that all the coefficients of the model are significant.
As a result of the calculation, the following model was obtained (in coded factors):

$$\Sigma\alpha=79{,}4+14{,}1T+4{,}9Mn+10{,}4Cr-1{,}4\cdot T\cdot Mn-7{,}4\cdot T\cdot Cr-13{,}1\cdot Mn\cdot Cr+8{,}1\cdot T\,Mn\cdot Cr. \quad (1)$$

Interpreting the resulting model, it can be concluded that the temperature has a predominant effect on the amount of α phase formed. In contrast, as the temperature decreases, the α↔β transformation occurs more fully, as well as the formation of the other intermetallic phases and double compounds. Moreover, with increasing both manganese and chromium, the amount of α phase increases, even as the temperature decreases. In this case, alloying with chromium has a predominant effect. Taking into account the rules for interpreting regression coefficients when assessing the paired effect of factors, to increase the amount of α phase, a multidirectional change in the number of alloying elements is necessary. In this case, this is probably caused by the concomitant effect of the amount of iron, which is not directly reflected in this model but participates in the formation of the phase composition through the accepted restrictions. The strengthening of the effect of simultaneous alloying with chromium and manganese is also indicated by the value of the coefficient for a paired combination of the factors of the chromium and manganese amount. In contrast, all the coefficients of the model with the participation of chromium are higher than those of the model with manganese. Based on the data obtained, it is preferable to alloy predominantly with chromium, with the simultaneous addition of a small amount of manganese. This is especially pronounced at low temperatures. Comparison of the results of co-alloying with the results of alloying with either manganese or chromium shows better results. In contrast, alloying schemes that retain iron at the level of ~20 % are preferable.

CONCLUSION

The features of alloying the iron- and silicon-rich alloy of the Al-Fe-Si system separately with manganese and chromium, as well as jointly with manganese and chromium, were studied. For this purpose, the ThermoCalc software was used. Possible conditions for the existence of the α phase were revealed, which are limited by the iron content of 24-39 %, the silicon content of 1-16 %, and the temperature of 770-425 °C. With a further decrease, a complete transformation of α↔β occurs. Additional doping with manganese and chromium expands the boundaries of the existence of the α phase by suppressing the α↔β transformation with the formation of cubic phases $\alpha_{Mn/Cr}$ when doped separately with manganese/chromium; when doped together, a complex cubic phase $Al_{15}Si_2(Fe,Cr,Mn)_4$ is formed. For the $Al_{60} – Fe_{30-x} – Si_{10} – Mn_x$ alloys, complete suppression of the β phase formation is achieved at 600 °C with the manganese content of more than 10 %, at the temperature of 500 °C from 15 % manganese; with decreasing the temperature the β phase is present in insignificant quantities. For the $Al_{60} – Fe_{30-x} – Si_{10} – Cr_x$ alloys, complete suppression of the β phase formation is achieved with the chromium content of more than 5% (at the temperature of 400 °C and with 5% chromium, there is observed 15 % of the β phase). Joint doping with manganese and chromium is more effective in suppressing the formation of the β phase, but doping schemes in which iron is maintained at a level of ~20% are preferable.

Acknowledgements: This research has been funded by the Science Committee of the Ministry of Science and Higher Education of the Republic of Kazakhstan (Grant No. AP19675471).

REFERENCES

1. P. Mikolajczak: Materials, 16 (9), 2023, 3304. https://doi.org/10.3390/ma16093304
2. V.A. Andreyachshenko, A.B. Naizabekov, Metalurgija, 55(3), 2016, 353–356.
3. V. Andreyachshenko, A. Toleuova: Kompleksnoe Ispolzovanie Mineralnogo Syra-Complex use of mineral resources, 332(1), 2025, 98-107. https://doi.org/10.31643/2025/6445.09
4. V. Andreyachshenko, I. Bartenev, Y. Malashkevichute-Brillant: Acta Metallurgica Slovaca, 30(3), 2024, 133-136. https://doi.org/10.36547/ams.30.3.2065
5. V. A. Andreyachshenko: Kovove Materialy-Metallic Materials, 60(2), 2022, 79–87. https://doi.org/10.31577/km.2022.2.79
6. C. G. McKamey, J. H. DeVan, P. F. Tortorelli, V. K. Sikka: Journal of Materials Research, 6, 2011, 1779–1805. https://doi.org/10.1557/JMR.1991.1779
7. S. Sampath, V.P. Ravi, S. Sundararajan: Crystals, 13(3), 2023, 435. https://doi.org/10.3390/cryst13030435
8. S. E. Haghighi, K. Janghorban: Journal of Alloys and Compounds, 495, 2010, 260–264. https://doi.org/10.1016/j.jallcom.2010.01.145
9. S. Ji, W. Yang, F. Gao: Transactions of Nonferrous Metals Society of China, 25(5), 2015, 1704–1714. https://doi.org/10.1016/S1003-6326(15)63776-1.
10. Z. Que, C. L. Mendis: Intermetallics, 127, 2020. 106960. https://doi.org/10.1016/j.intermet.2020.106960
11. M. V. Canté, T. S. Lima, C. Brito, A. Garcia, N. Cheung, J. E. Spinelli: Journal of Sustainable Metallurgy, 4, 2018, 412–426. https://doi.org/10.1007/s40831-018-0188-y
12. X. Zhang, D. Wang, X. Li, H. Zhang, H. Nagaumi: Intermetallics, 131, 2021, 107103. https://doi.org/10.1016/j.intermet.2021.107103
13. P. Orozco-González, M. Castro-Román, R. Muñiz-Valdez, S. Luna-Álvarez, F. Equihua-Guillén, A. Hernández-Rodríguez, V. H. Baltazar-Hernández, F. Alvarado-Hernández: Materials Letters, 180, 2016, 277–279. https://doi.org/10.1016/j.matlet.2016.05.139
14. L. Jin, K. Liu, X. Grant Chen: Materials Science and Engineering: A, 770, 2020, 138554. https://doi.org/10.1016/j.msea.2019.138554
15. B. Wang, J. Wang, X. Liu, Q. Li, X. Liu: Materials Science and Engineering: A, 858, 2022, 144090. https://doi.org/10.1016/j.msea.2022.144090
16. J. M. Yu, N. Wanderka, A. Rack, R. Daudin, E. Boller, H. Markötter, A. Manzoni, F. Vogel, T. Arlt, I. Manke, J. Banhart: Journal of Alloys and Compounds, 766, 2018, 818–827. https://doi.org/10.1016/j.jallcom.2018.06.372
17. X. Wu, H. Zhang, F. Zhang, Z. Ma, L. Jia, B. Yang, T. Tao, H. Zhang: Materials Characterization, 139, 2018, 116–124. https://doi.org/10.1016/j.matchar.2018.02.029
18. H. Becker, T. Bergh, P. E. Vullum, A. Leineweber, Y. Li: Materialia, 5, 2019, 100198. https://doi.org/10.1016/j.mtla.2018.100198
19. W.-ch. Yang, F. Gao, S.-x. Ji: Transactions of Nonferrous Metals Society of China, 25(5), 2015, 1704–1714. https://doi.org/10.1016/S1003-6326(15)63776-1
20. V.A. Andreyachshenko, Y.I. Malashkevichute-Brillant: Kompleksnoe Ispolzovanie Mineralnogo Syra, 336(1), 2026, 105–113. https://doi.org/10.31643/2026/6445.10
21. J. M. Yu, N. Wanderka, G. Miehe, J. Banhart: Intermetallics, 72, 2016, 53–61. https://doi.org/10.1016/j.intermet.2016.02.003
22. V. A. Andreyachshenko, M. K. Ibatov: Metallurgical Research & Technology, 121(3), 2024, 315. https://doi.org/10.1051/metal/2024035
23. A. Hernández-Rodríguez, M. D. J. Castro-Román, M. Herrera-Trejo, S. Belmares-Perales, P. Orozco-González: Metalurgija, 53(3), 2014, 314–316.
24. R. Podprocká, D. Bolibruchová: Archives of Foundry Engineering, 18(2), 2018, 95–99. https://doi.org/10.24425/122508
25. D. Bolibruchova, A. Ivanova: Archives of Foundry Engineering, 19(3), 2019, 15–20. https://doi.org/10.24425/afe.2019.127129
26. D. Song, Y. Jia, Q. Li, Y. Zhao, W. Zhang: Materials, 15(4), 2022, 1618. https://doi.org/10.3390/ma15041618
27. R. Kakitani, A. V. Rodrigues, C. Silva, A. Garcia, N. Cheung: Journal of Alloys and Metallurgical Systems, 1, 2023, 100005. https://doi.org/10.1016/j.jalmes.2023.100005
28. A. Bjurenstedt, D. Casari, S. Seifeddine, R. H. Mathiesen, A. K. Dahle: Acta Materialia, 130, 2017, 1–9. https://doi.org/10.1016/j.actamat.2017.03.026
29. N. Pang, Z. Shi, C. Wang, N. Li, Y. Lin: Materials, 14(4), 2021, 768. https://doi.org/10.3390/ma14040768
30. E. de Rosso, C. A. dos Santos, A. Garcia: Advanced Engineering Materials, 24(8), 2022, 2001552. https://doi.org/10.1002/adem.202001552